# Developing a fishery-independent index of relative abundance for Gulf of Mexico Brown Shrimp using VAST

Lisa Ailloud, Molly Stevens, Brendan Turley, Adam Pollack, and David Hanisko

SEDAR87-AP-03

31 January 2025

*This information is distributed solely for the purpose of pre-dissemination peer review. It does not represent and should not be construed to represent any agency determination or policy.*

Please cite this document as:

Ailloud, Lisa, Molly Stevens, Brendan Turley, Adam Pollack, and David Hanisko. 2025. Developing a fishery-independent index of relative abundance for Gulf of Mexico Brown Shrimp using VAST. SEDAR87-AP-03. SEDAR, North Charleston, SC. 26 pp.

# Developing a fishery-independent index of relative abundance for Gulf of Mexico Brown Shrimp using VAST.

Lisa Ailloud[1], Molly Stevens[2], Brendan Turley[3], Adam Pollack[4], and David Hanisko[4]
[1]*Southeast Fisheries Science Center (SEFSC), National Marine Fisheries Service (NMFS), National Oceanographic and Atmospheric Administration (NOAA), Charleston SC, USA*
[2]*SEFSC, NMFS, NOAA, St. Petersburg FL, USA*
[3]*Cooperative Institute of Marine and Atmospheric Studies; University of Miami, Miami, FL*
[4]*SEFSC, NMFS, NOAA, Pascagoula, MS, USA*

## 1. Introduction

Brown shrimp (*Farfantepenaeus aztecus*) indices of relative abundance were developed for consideration in the SEDAR 87 Gulf of Mexico (GOM) white, pink, and brown shrimp stock assessment process for input into JABBA, a Bayesian state-space surplus production modelling tool (Winker, Carvalho, and Kapur 2018).

Shrimp indices of abundance have historically been developed using standard delta-lognormal GLM approaches applied to data from the Southeast Area Monitoring and Assessment Program (SEAMAP) Groundfish Surveys (1987-present). Summer and Fall survey data have typically been used separately when developing indices, with a split in the middle of each time series (2007/08 for Fall and 2008/09 for Summer) when major changes in sampling design occurred (see *Methods* section below). For shrimp, the timing of the design break coincides with a period of unprecedented change in the fishery landscape likely to have impacted abundance. Between 1978 and 2002, Gulf-wide offshore shrimping effort was relatively stable. However, from 2003 to 2008, adverse economic conditions caused the fishery to consolidate and effort to drop dramatically (~70%) and stabilize at a new low level that is still being observed today. We were therefore motivated to find a modeling solution for linking the old and new SEAMAP survey design time series when generating an index of relative abundance for stock assessment. In addition, the SEAMAP Summer survey was originally designed to occur prior to the Texas Closure opening – a seasonal closure that takes place roughly May 15-July 15 of each year where Texas waters are closed to shrimp trawling to allow shrimp to reach larger sizes before harvest. However, in recent years, logistical constraints (e.g., vessel outages, inclement weather) have caused delays in the survey on several occasions (*Figure 1*). Given the potential impact that the timing of the survey relative to the Texas Closure and shrimp migration patterns could have on observed CPUE, we deemed it important to try and account for these spatiotemporal gaps and shifts in operation when developing the index of relative abundance.

To that end, we used the Vector Autoregressive Spatio-Temporal (VAST) modeling platform to develop a single, continuous standardized index of abundance for brown shrimp. VAST is an R package for implementing a spatial delta-generalized linear mixed model (delta-GLMM) when standardizing survey data. It allows for predicting population density based on both habitat covariates (i.e., covariates that affect population density) and spatial and spatiotemporal random effects. This flexible framework capable of accounting for changes in the spatiotemporal footprint of surveys through time also allows for integrating data from multiple surveys given sufficient spatiotemporal overlap between the surveys. For brown shrimp, both the SEAMAP surveys (Summer and Fall) and the Texas Parks and Wildlife Department (TPWD) Gulf survey (SEDAR 2024a) were used for developing a single, joint index of relative abundance for the stock. There was interest in using the Texas survey in concert with SEAMAP because the Texas survey operates monthly and could therefore provide information on intra-annual changes in shrimp abundance off the coast of Texas to help correct any bias that might arise from changes in the timing of the SEAMAP survey relative to the Texas Closure. Lastly, many studies point to the fact that environmental conditions (e.g., salinity and temperature) in the nursery grounds play an important role in driving the abundance and distribution of shrimp each year. We further explored whether the inclusion of environmental covariates could help explain the variability observed in the index through the use of habitat covariates in VAST.

This paper details the data, workflow, and results of applying the VAST modeling approach to Gulf of Mexico brown shrimp data to produce an index of relative abundance for the stock.

## 2. Methods

### 2.1 Stock description

Brown shrimp in the GOM range from the Florida Keys along the Gulf Coast to northwestern Yucatan in Mexico (SEDAR 2024b). Adults spawn offshore in the winter, and their larvae settle into nearshore estuarine or marsh nursery habitat in the spring. They then migrate back offshore a few months later as subadults where they become vulnerable to the fishery. Brown shrimp have a short life span of less than 2 years, and have a distinctive behavior of burrowing during the day and emerging in the water column at night (*Figure 2*), which is typically when the fishery operates (SEDAR 2024b). The bulk of the US Gulf of Mexico brown shrimp catches occur in the north and northwestern Gulf of Mexico (Williams et al. 2024).

### 2.2 Data

#### 2.2.1 Fishery Independent Surveys

A number of fishery-independent survey data time series were made available for SEDAR 87, and vetted during the Data Workshop (see Data Workshop Report (SEDAR 2024a) for more detail). Two data sources were retained for developing the index of relative abundance for the stock: the SEAMAP Groundfish survey and the Texas Parks and Wildlife Department (TPWD) Gulf survey.

The SEAMAP Groundfish survey is characterized by a 42 ft otter trawl that operates in the summer (typically June-July) and fall (typically October-November) of each year, towing both during the day and night. The time series extends from 1987 to 2022 but underwent major changes in sampling design following the 2008 Summer survey (SEDAR 2023a). Survey design changes included :

- a spatial expansion to the East (old design covered shrimp statistical grids 10-21; new design covered grids 1-21),
- a change from variable tow times (10-55 min) to fixed tow times (30 min),
- a change from towing across depth zones to not having any pre-defined tow direction,

- dropping the day/night stratification, and
- a change in the effort allocation through space which resulted in major changes in the effort distribution relative to different statistical zones and depth zones between the old and the new survey (SEDAR 2023b).

The spatial expansion to the East was a non-issue for brown shrimp : the bulk of the stock is located in the West so index development was restricted to statistical zones 11-21 over the depth zones covered by the TPWD (1.2-30m) and SEAMAP surveys (10-110m). Personal communication with the SEAMAP crew indicated that gear saturation was not an issue for any of the tows carried out on the survey. As such, the change from variable tow times to fixed tow times was taken into account in the modeling process by allowing for a linear offset of effort in minutes. The change in tow direction was also not assumed to have an appreciable impact on catch rates given the short distances / small changes in depth covered by singular tows. Given the diurnal burrowing behavior of brown shrimp, the time of day (day vs. night) was expected to impact catch rates. Time of day was accounted for in the modeling process by including a categorical catchability covariate. Lastly, with changes in the spatial distribution of sampling effort between the old and new survey, both East-West and North-South were expected to impact catch rates through time and were accounted for in the modeling process by estimating spatial and spatiotemporal variation in shrimp density through the use of random effects (RE).

The second survey used was the Texas Parks and Wildlife Department (TPWD) Gulf survey. The survey covers the same time span as SEAMAP (1987-2022) but takes place monthly at the mouth of five major TX bays that Brown shrimp use as nursery grounds (Parks and Wildlife Division 2023). Sixteen samples are collected every month in each of the five areas within the Texas Territorial Sea (shoreline to nine nautical miles offshore). Trawls are 20 ft wide otter trawls with 38 mm (1.5 in) stretched nylon multifilament mesh throughout. Sampling takes place during the daytime, trawls are towed parallel to the fathom curve and all tow times are 10 minutes in duration.

The two surveys overlap at the mouth of major TX bays and shallowest edge of the SEAMAP survey between 5 and 9 fathoms. The joint analysis of the two datasets was motivated by the fact that the Texas survey operates monthly and could therefore provide information on intra-annual changes in shrimp abundance off the coast of Texas to help correct any bias that might arise from changes in the timing of the SEAMAP survey.

**2.2.2 Time Series of Environmental Data**

Indices of mean annual temperature and salinity in the nursery grounds were developed by Turley, Ailloud, and Stevens (2023), and used to test the impact of environmental conditions on stock abundance. These indices were constructed based on the timing and regions that are thought to supply the bulk of the commercial catches for brown shrimp to capture the variability and trends of the environmental drivers (salinity and temperature) that are most likely to influence recruitment success and, as a result, exploitable biomass. These indices were input into VAST as habitat covariates to test whether their inclusion helped explain a portion of the year-to-year variability observed in the index of relative abundance. A set of lagged indices (one and two years) were also tested. The median of the time series was used as substitutes for the initial years that preceded lagged data availability (i.e. 1987 for the 1-year lag time series and 1987-1988 for the 2-year lag time series).

## 2.3 Modeling Approach

### 2.3.1 Model Description

We used the Vector Autoregressive Spatiotemporal (VAST) model v3.11.0 (J. T. Thorson and Barnett 2017) implemented in R v.4.4.0 (R Core Team, 2020) to develop indices of relative abundance for each stock. This spatial-delta generalized linear mixed effects model is defined by two linear predictors : $p_1$ to calculate encounter probabilities (or zero-inflation probabilities in a count-data model) and $p_2$ for positive catch rates in numbers of shrimp per tow (or the count-data intensity function in a count-data model) for each observation $i$ at location $s_i$ and time $t_i$.

$$p_1(i) = \beta_1(t_i) + \omega_1^*(s_i) + \epsilon_1^*(s_i, t_i) + \gamma_1(t_i) + \lambda_1(i)$$

$$p_2(i) = \beta_2(t_i) + \omega_2^*(s_i) + \epsilon_2^*(s_i, t_i) + \gamma_2(t_i) + \lambda_2(i)$$

Where $\beta$ are the year intercepts for each linear predictor (temporal variation, fixed effect), $\omega^*$ are the spatial factors (random effects), $\epsilon^*$ are the spatio-temporal factors (random effects), $\gamma$ represent the impacts of habitat covariates on each linear predictor and $\lambda$ represent the impacts of catchability covariates on each linear predictor. Linear predictors are then transformed to predict encounter probabilities and positive catch rates. In the case of a conventional delta-model :

$$r_1 = logit^{-1}\big(p_1(i)\big)$$

$$r_2 = a_i * exp\big(p_2(i)\big)$$

where $a_i$ is the effort offset (in minutes fished). Then, VAST predicts population density $d(s,t)$ at extrapolation grids across a continuous spatial domain (pre-defined to cover the extent of the surveys) and discrete time intervals (years) from both transformed linear predictors as (in the case of a conventional delta-model):

$$d(s,t) = logit^{-1}\big(\beta_1(t_i) + \omega_1^*(s_i) + \epsilon_1^*(s_i, t_i) + \gamma_1(t_i)\big) * exp\big(\beta_2(t_i) + \omega_2^*(s_i) + \epsilon_2^*(s_i, t_i) + \gamma_2(t_i)\big)$$

and calculates the abundance index $I(t)$ in time $t$ as :

$$I(t) = \sum_{s=1}^{n_s} \big(a(s) * d(s,t)\big)$$

where $a(s)$ is the area associated with knot $s$. Habitat covariates are processes that affect true underlying densities, they are used in both the fitting process and the prediction process. Catchability covariates are processes that affect sampling but do not reflect underlying densities, their estimated effect is removed when calculating the index. Estimates of "density" for brown shrimp are not directly interpretable on an absolute scale as no meaningful estimate of area swept could be produced for these surveys.

Spatial and spatiotemporal variation are estimated using Gaussian Markov random fields (J. T. Thorson 2019a). The spatial correlation matrix is modeled using a Matérn covariance function (Lindgren, Rue, and Lindström 2011). The user can specify a Matérn covariance function that is either isotropic (where correlations decline at the same rate in any direction) or anisotropic (where the rate at which correlations decline depends upon the direction of movement – common in marine ecosystems, where correlations decline slowly when moving along a depth contour but rapidly when moving perpendicular to the depth contour (J. T. Thorson 2019a)). The number of prediction locations (i.e. knots) must be predefined. VAST then distributes the knots spatially using a k-means algorithm that minimizes the average distance between samples and knots. A detailed description of the model can be found in (J. T. Thorson 2019b) and in the VAST User Manual (J. Thorson 2024).

**2.3.2 Prediction grid**

Before fitting VAST models, we constructed prediction grids for the study species. A 3km x 3km extrapolation grid was constructed to encompass the total area covered by both surveys (*Figure 3*).

**2.3.3 Modeling Workflow**

Model development involved the following steps:

1. *Selecting the optimal number of knots :* a delta-lognormal model with both spatial and spatiotemporal random effects and no habitat or catchability covariates was run using a series of knots from 250 to 1500 knots to determine the optimal number of knots to use while balancing computational speed and spatial resolution. The root mean square error (RMSE) between raw observations and fitted values of the index was used to measure differences between runs and find the number of knots beyond which results appeared to stabilize.

2. *Identifying the optimal distribution model :* Candidate models included :

    – a Poisson-link delta-model (*ObsModel=c(2,1)*) : log-linked linear predictor for encounter probability (i.e., Poisson), and a gamma error distribution for positive catch rates;

    – a Zero-inflated negative binomial model (*ObsModel=c(5,0)*) : 1st linear predictor for logit-linked zero-inflation, 2nd linear predictor for log-linked conditional mean of negative binomial;

    – a Conventional lognormal delta-model (*ObsModel=c(4,0)*) : logit-link for encounter probability and log-link for positive catch rates.

    Standard model selection tools (i.e., AIC, qq plots) were used to identify the best fitting model.

3. *Testing the inclusion of spatial and spatiotemporal random effects :* Using the optimal number of knots and distribution function determined in steps 1. and 2., a series of models were built with increasing complexity with respect to including spatial and spatiotemporal random effects. If the estimated variances of the spatial and spatiotemporal terms were greater than zero, the random effects were retained. Random effects, when present, were included in both linear predictors. AIC was used to select the Matérn covariance functions (anisotropic vs. isotropic).

4. *Selecting catchability covariates :* Using the optimal model determined in step 3., we explored the impact of including the following catchability covariates: survey, time of

day (tod) and month. Catchability covariates were included in both linear predictors. AIC was used to assess model fit.

5. *Selecting habitat covariates :* Using the optimal model determined in step 4., we explored the impact of including the following habitat covariates: indices of mean annual temperature and salinity in the nursery grounds and these same indices lagged by 1 and 2 years. Indices were normalized to a mean of zero and standard deviation of 1 prior to input into the model and set up as spatially explicit annual zero-centered covariates to predict changes in density across space and time (i.e., single value across space within a year but varied from year to year). Habitat covariates were included in both linear predictors. AIC was used to assess model ($m$) fit. Following (Cao et al. 2017), a pseudo-$R^2$ metric was calculated to determine the proportion of variance ($\sigma^2$) from the null model ($null$; i.e., habitat covariates) that was explained by including habitat variables :

$$pseudo - R^2 = 1 - \frac{\sigma^2_{\omega,m} + \sigma^2_{\epsilon,m}}{\sigma^2_{\omega,null} + \sigma^2_{\epsilon,null}}$$

## 3. Results

1. *Selecting the optimal number of knots :* The RMSE reached an asymptote around 700 knots (*Figure 4*) and there was very little difference in the estimated index using 700 (runtime : 1.4hrs) vs. 1500 knots (run time : 5.6hrs) (*Figure 5*). A model with 700 knots was therefore retained for subsequent model building steps.

2. *Identifying the optimal distribution model :* The zero-inflated negative binomial model did not converge. Comparing the poisson-link delta-model (VAST default option) with the conventional lognormal delta-model, AIC and qqplots indicated that the delta-lognormal model was preferred (*Figure 6*).

3. *Testing the inclusion of spatial and spatiotemporal random effects :* The marginal standard deviation of both spatial ($\omega$) and spatiotemporal ($\epsilon$) random effects were significantly greater than zero and thus included in the final model ($\omega_1 = 1.94$; $\omega_2 = 0.82$; $\epsilon_1 = 0.48$; $\epsilon_2 = 0.73$). The model that assumed anisotropic covariance was favored in terms of AIC (*Table 1*, *Figure 7*). Including spatial random effects alone brought significant improvements to the model fit.

4. *Selecting catchability covariates :* The model with the lowest AIC was the model that included time of day, survey and month as catchability covariates (*Table 2*). Month had the largest effect, followed by time of day (*Figure 8*). The fixed effect for survey (Q) had only a minor impact on the overall fit. Effects plots for time of day and month are shown in *Figure 9* and *Figure 10*.

5. *Selecting habitat covariates :* The model with the lowest AIC was the model that included the average nursery temperature index with no lags as habitat covariate (*Table 3*). However, it resulted in a nearly identical fit as the null model with no habitat covariates ($\Delta AIC = 13$ ; *Figure 11*) and only explained a trivial fraction (<2%) of the spatial and spatiotemporal variation observed. None of the habitat covariates explained any considerable amount of spatial or spatiotemporal variation in the model.

The final model included spatial and spatiotemporal random effects using the anisotropic estimation of correlation (*Figure 12*), and catchability covariates survey, time of day, and month, in both the 1st and 2nd linear predictors. The use of spatial REs had the largest effect in the standardization process. None of the habitat covariates had an appreciable impact on the index trend and each explained only a very small portion of the variance from the null model with no habitat covariates. Because of that and the fact that this index is meant for assessment purposes and benefits from being simple to update, the final model did not include any habitat covariates. *Figure 13* shows the final standardized index plotted against the non-standardized index. The distribution of quantile residuals did not show any substantial spatial pattern (*Figure 14*). The model fit the data reasonably well (*Figure 15*).

## 4. Discussion

The standardization process resulted in an index with an, overall, steeper increase across the time series (*Figure 13*). Index values associated with the old survey design generally fell below the nominal values and index values associated with the new survey design generally fell above. When the survey switched from the old to the new survey design, more effort shifted towards statistical zones 16-19 (18-19 being areas with relatively higher brown shrimp densities) with some effort shifting away from statistical zone 11 (area with relatively lower brown shrimp densities). In terms of depth, the original effort allocation was approximately 1/3 for depths less than 20 fathom and 2/3rd for depth greater than 20 fathoms. After the design change a greater portion of effort shifted to the larger depths in statistical zone 13-21, where brown shrimp are found in higher densities. Those two spatial shifts combined would be expected to yield higher CPUEs under the new design compared to the old design, which is in line with what the standardization process achieved. Similarly, in recent years in which the Summer SEAMAP survey was late to operate (i.e., 2021-2022), the predicted index was significantly higher than the observed nominal CPUE. This result was in line with our intuition that the later the survey operates, the more likely the observed CPUE is to be biased low as more fishing has occured.

Average salinity and temperature in the nursery grounds were not found to have an appreciable impact on spatial variation in shrimp density. While many studies point to the relationship between shrimp production and temperature and salinity on the nursery grounds (see SEDAR (2024c)), it is likely that averaging conditions over a large scale, as we did here, masks our ability to detect a strong signal. The indices were developed by averaging conditions across Texas and Lousiana based on the spatial extent of nursery habitat. Yet, it is more likely that not all nursery grounds are created equal such that certain estuaries contribute much more to the overall GOM shrimp production than others due to factors other than spatial extent. It is also likely that the relationship between CPUE and environmental conditions is not linear and would be better described using a spline where shrimp production is maximized under certain conditions but hampered under extremes. At the time that this work was conducted, it was not possible in VAST to specify a more complex relationship for the environmental index so that option was not explored.

The final model including spatial and spatiotemporal random effects and catchability covariates survey, time of day, and month, for both the 1st and 2nd linear predictors but no habitat covariate is recommended as the index for input into JABBA.

## References

Cao, Jie, James T. Thorson, R. Anne Richards, and Yong Chen. 2017. "Spatiotemporal Index Standardization Improves the Stock Assessment of Northern Shrimp in the Gulf of Maine." *Canadian Journal of Fisheries and Aquatic Sciences* 74 (11): 1781–93. *https://doi.org/10.1139/cjfas-2016-0137*.

Lindgren, Finn, Håvard Rue, and Johan Lindström. 2011. "An Explicit Link Between Gaussian Fields and Gaussian Markov Random Fields: The Stochastic Partial Differential Equation Approach." *Journal of the Royal Statistical Society Series B: Statistical Methodology* 73 (4): 423–98. *https://doi.org/10.1111/j.1467-9868.2011.00777.x*.

Parks, Texas, and Wildlife Division. 2023. "TPWD's Gulf Trawl Sample Design." *https://sedarweb.org/documents/sedar-87-rd07-tpwds-gulf-trawl-sample-design/*.

SEDAR. 2023b. "SEAMAP Trawl Shrimp Data and Index Estimation Work Group Report." North Charleston, SC. *https://sedarweb.org/documents/sedar-rd01-seamap-trawl-shrimp-data-and-index-estimation-work-group-report/*.

SEDAR. 2023a. "SEAMAP Trawl Shrimp Data and Index Estimation Work Group Report." North Charleston, SC. *https://sedarweb.org/documents/sedar-rd01-seamap-trawl-shrimp-data-and-index-estimation-work-group-report/*.

SEDAR. 2024b. "SEDAR 87 Gulf of Mexico White, Pink, and Brown Shrimp SECTION II: Data Workshop Report." SEDAR. *https://sedarweb.org/documents/sedar-87-gulf-of-mexico-white-pink-and-brown-shrimp-data-workshop-report/*.

SEDAR. 2024a. "SEDAR 87 Gulf of Mexico White, Pink, and Brown Shrimp SECTION II: Data Workshop Report." *https://sedarweb.org/documents/sedar-87-gulf-of-mexico-white-pink-and-brown-shrimp-data-workshop-report/*.

SEDAR. 2024c. "SEDAR 87 Gulf of Mexico White, Pink, and Brown Shrimp SECTION II: Data Workshop Report." *https://sedarweb.org/documents/sedar-87-gulf-of-mexico-white-pink-and-brown-shrimp-data-workshop-report/*.

Thorson, James. 2024. "VAST Manual." *https://github.com/James-Thorson-NOAA/VAST/blob/main/manual/VAST_model_structure.pdf*.

Thorson, James T. 2019a. "Guidance for Decisions Using the Vector Autoregressive Spatio-Temporal (VAST) Package in Stock, Ecosystem, Habitat and Climate Assessments." *Fisheries Research* 210 (February): 143–61. *https://doi.org/10.1016/j.fishres.2018.10.013*.

Thorson, J. 2019b. "Guidance for Decisions Using the Vector Autoregressive Spatio-Temporal (VAST) Package in Stock, Ecosystem, Habitat and Climate Assessments." *Fisheries Research* 210 (February): 143–61. *https://doi.org/10.1016/j.fishres.2018.10.013*.

Thorson, James T., and Lewis A. K. Barnett. 2017. "Comparing Estimates of Abundance Trends and Distribution Shifts Using Single- and Multispecies Models of Fishes and Biogenic Habitat." Edited by Emory Anderson. *ICES Journal of Marine Science* 74 (5): 1311–21. *https://doi.org/10.1093/icesjms/fsw193*.

Turley, Brendan, Lisa Ailloud, and Molly Stevens. 2023. "Development of Estuarine Environmental Indices for SEDAR 87 Gulf of Mexico White, Pink, and Brown Shrimp Stock Assessment." North Charleston, SC. *https://sedarweb.org/documents/sedar-87-ap-01-development-of-estuarine-environmental-indices-for-sedar-87-gulf-of-mexico-white-pink-and-brown-shrimp-stock-assessment/*.

Williams, Jo, Kimberly Johnson, Kyle Detloff, and Alan Lowther. 2024. "SEDAR 87 Commercial Fishery Landings and Effort Figures for White, Pink, and Brown Shrimp in the US Gulf of Mexico, 1960-2022." North Charleston, SC. *https://sedarweb.org/documents/sedar-84-dw-16-sedar-84-commercial-fishery-landings-and-effort-figures-for-white-pink-and-brown-shrimp-in-the-us-gulf-of-mexico-1960-2021/*.

Winker, Henning, Felipe Carvalho, and Maia Kapur. 2018. "JABBA: Just Another Bayesian Biomass Assessment." *Fisheries Research* 204 (August): 275–88. *https://doi.org/10.1016/j.fishres.2018.03.010*.

## Tables

| Run Description | $\sigma_{\omega 1}$ | $\sigma_{\omega 2}$ | $\sigma_{\varepsilon 1}$ | $\sigma_{\varepsilon 2}$ | AIC | ΔAIC |
|---|---|---|---|---|---|---|
| No RE | | | | | 250,341 | 21,166 |
| Spatial RE (iso) | 1.96 | 0.81 | | | 230,465 | 1,290 |
| Spatial (iso) & spatiotemporal REs | 1.86 | 0.79 | 0.47 | 0.72 | 229,200 | 25 |
| **Spatial (aniso) & spatiotemporal REs** | **1.94** | **0.82** | **0.48** | **0.73** | **229,175** | **0** |

Table 1. Marginal standard deviation of spatial ($\omega$) and spatiotemporal ($\epsilon$) terms and AIC across runs with different specifications for the spatial and spatiotemporal random effects and associated Matérn covariance function. The run with the lowest AIC is bolded. *RE: random effects; iso : isotropic Matérn covariance function; aniso: anisotropic Matérn covariance function.*

| Run Description | $\sigma_{\omega 1}$ | $\sigma_{\omega 2}$ | $\sigma_{\varepsilon 1}$ | $\sigma_{\varepsilon 2}$ | AIC | ΔAIC |
|---|---|---|---|---|---|---|
| Null model | 1.94 | 0.82 | 0.48 | 0.73 | 229,175 | 13,110 |
| **Saturated model** | **1.87** | **0.88** | **0.69** | **0.71** | **216,065** | **0** |
| Saturated model - Q | 2.07 | 0.89 | 0.69 | 0.71 | 216,474 | 409 |
| Saturated model - tod | 1.70 | 0.73 | 0.65 | 0.80 | 219,930 | 3,865 |
| Saturated model - month | 1.67 | 0.89 | 0.53 | 0.67 | 224,138 | 8,073 |
| Null model + month | 1.97 | 0.78 | 0.62 | 0.78 | 221,075 | 5,010 |
| Null model + tod | 2.01 | 0.91 | 0.54 | 0.67 | 224,859 | 8,794 |
| Null model + Q | 1.54 | 0.75 | 0.50 | 0.74 | 227,541 | 11,476 |

Table 2. Marginal standard deviation of spatial ($\omega$) and spatiotemporal ($\epsilon$) terms and AIC across runs with different specifications for the catchability covariates. The run with the lowest AIC is bolded.

| Run Description | $\sigma_{\omega 1}$ | $\sigma_{\omega 2}$ | $\sigma_{\varepsilon 1}$ | $\sigma_{\varepsilon 2}$ | $pseudoR^2_1$ | $pseudoR^2_2$ | AIC | ΔAIC |
|---|---|---|---|---|---|---|---|---|
| Null model | 1.87 | 0.88 | 0.69 | 0.71 | 0.000 | 0.000 | 216,065 | 13 |
| **Null model + temperature** | **1.87** | **0.88** | **0.69** | **0.69** | **0.001** | **0.019** | **216,052** | **0** |
| Null model + salinity | 1.87 | 0.88 | 0.69 | 0.71 | 0.000 | 0.002 | 216,067 | 15 |
| Null model + temperature (lag=1) | 1.87 | 0.88 | 0.69 | 0.70 | 0.000 | 0.006 | 216,064 | 12 |
| Null model + salinity (lag=1) | 1.87 | 0.88 | 0.69 | 0.71 | 0.000 | 0.000 | 216,067 | 15 |
| Null model + temperature (lag=2) | 1.87 | 0.88 | 0.69 | 0.71 | 0.000 | 0.002 | 216,067 | 15 |
| Null model + salinity (lag=2) | 1.87 | 0.88 | 0.69 | 0.71 | 0.000 | 0.000 | 216,067 | 15 |

Table 3. Marginal standard deviation of spatial ($\omega$) and spatiotemporal ($\epsilon$) terms and pseudo-R2 showing the proportion of variance from the null model (i.e., the model with no habitat covariates included) that is explained by including habitat covariate(s) in the model. The run with the lowest AIC is bolded.

## Figures


Figure 1: Spatiotemporal footprint of the SEAMAP Summer and Fall Surveys through time. The colors are indicative of the different shrimp statistical zones ("statzone") and the shapes refer to the U.S. Gulf of Mexico states associated with stations sampled within each of these zones. Red reference lines mark the break in the survey design.

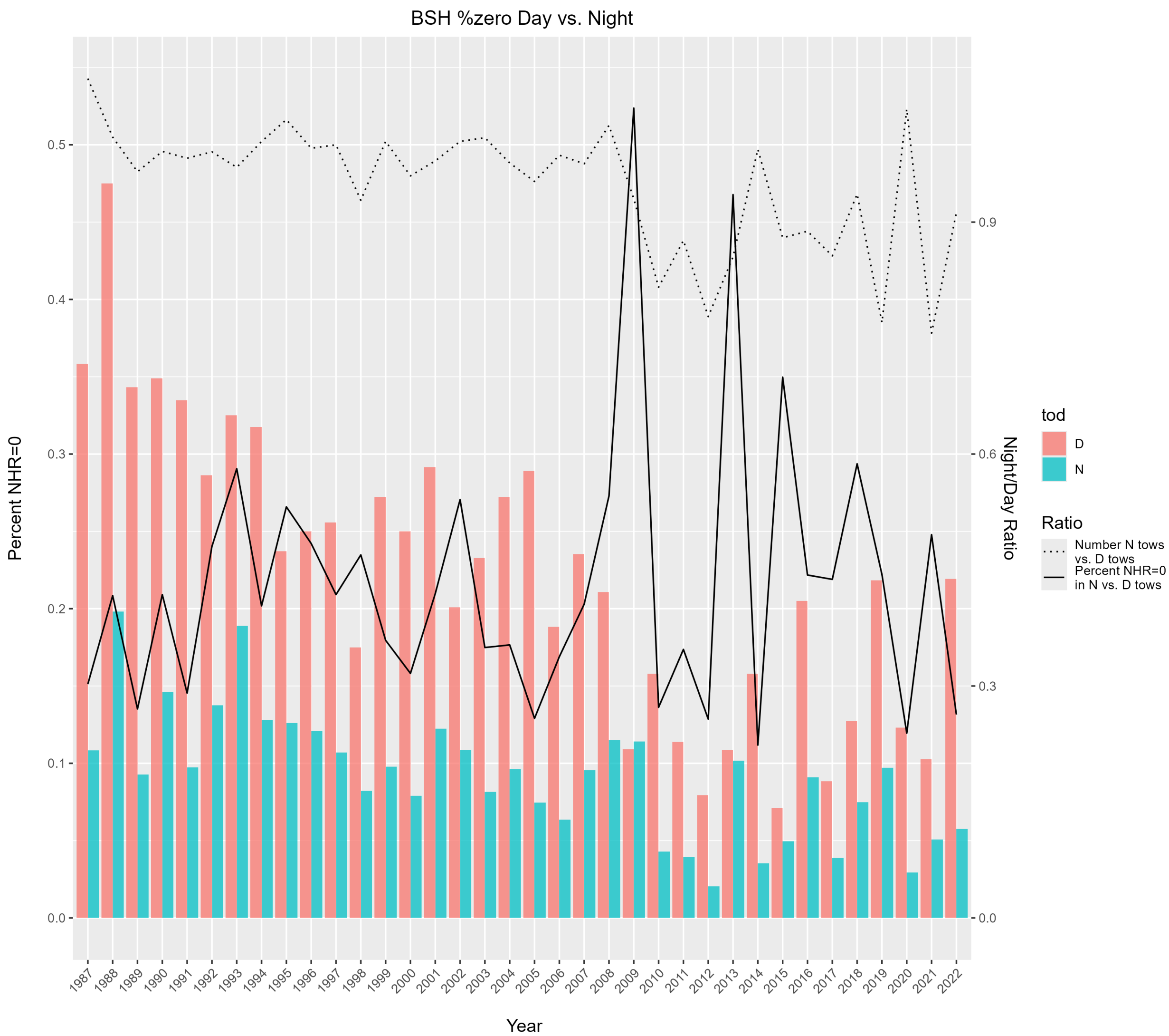


Figure 2: Barplot comparing the fraction (between 0 and 1) of SEAMAP tows with zero catch (NHR = numbers per hour) between daytime (D) and nightime (N) tows (primary y axis). The ratio of zero catch tows during the night vs. day is shown in the black solid line (secondary y axis). The ratio of the number of tows conducted at night vs. during the day is shown in the dashed line (secondary y axis). The ~50:50 split imposed by the old survey design shifts towards more daytime tows after 2008/2009.

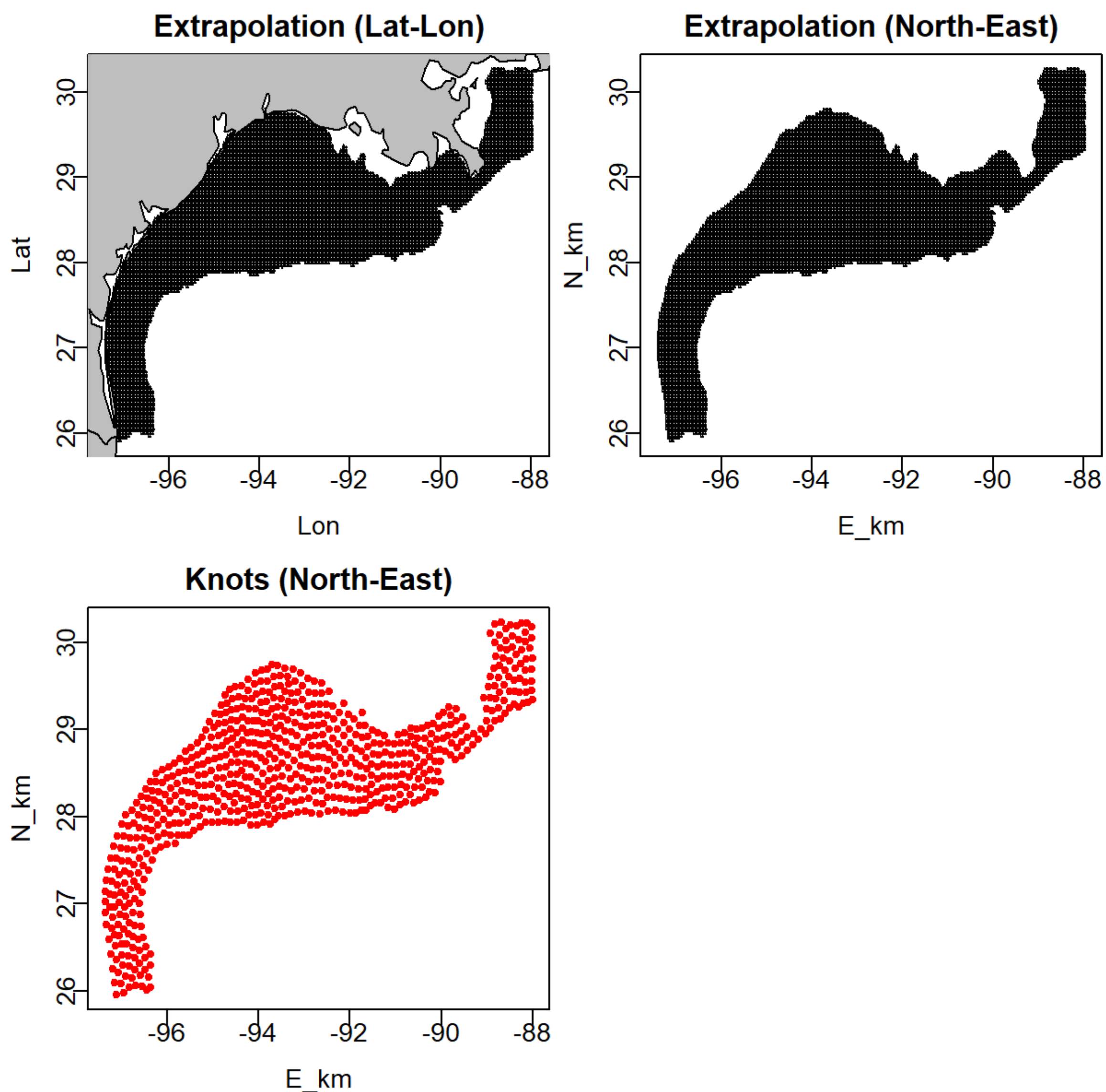


Figure 3: Gulf of Mexico extrapolation region (top panels). For computational efficiency, 700 knots were specified to approximate the spatial and spatiotemporal variation terms of the spatiotemporal model developed in this study (bottom panel).

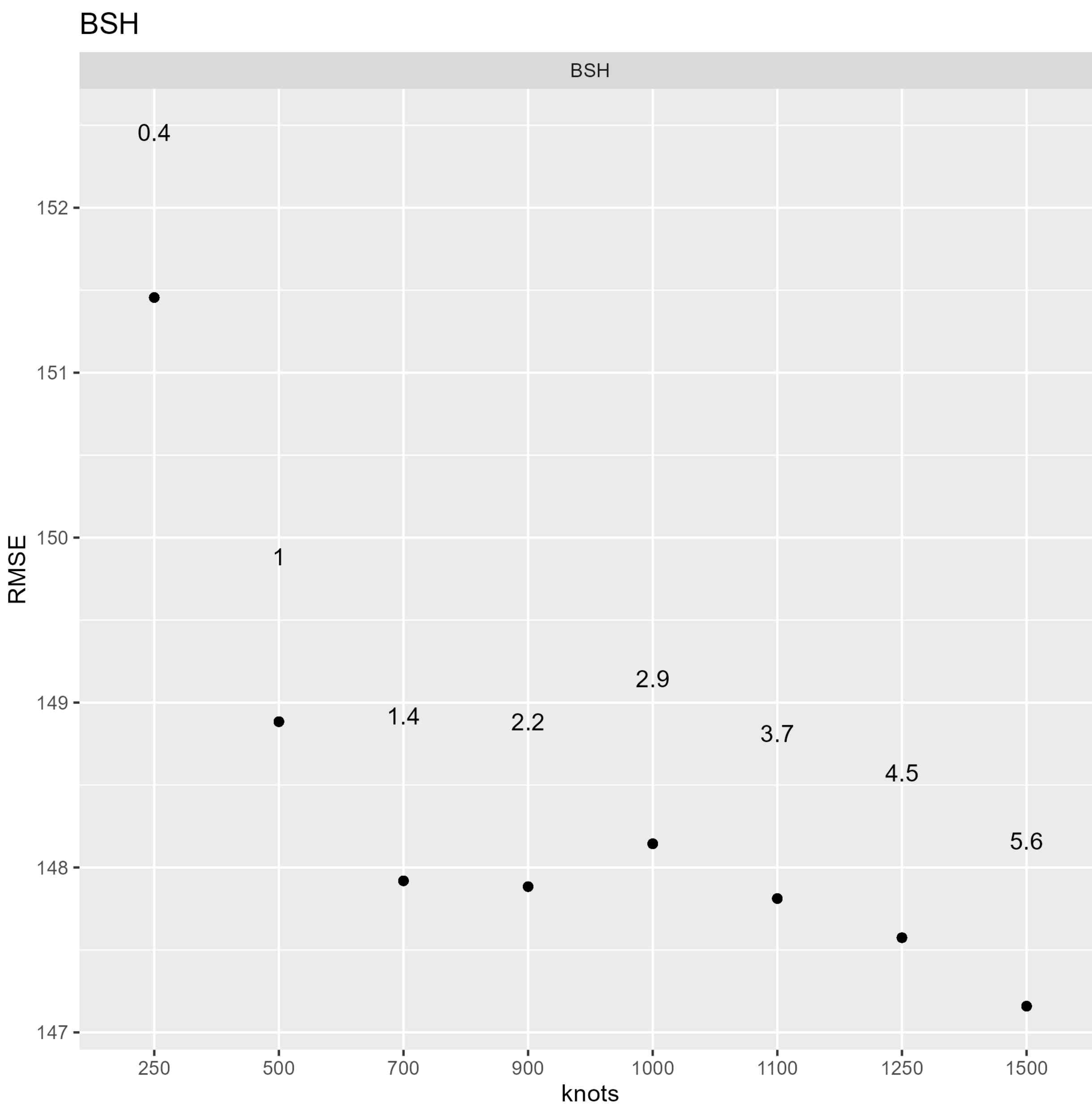


Figure 4: Index RMSE associated with each model run for the different numbers of knots attempted. Run time in hours is printed above each data point. Increasing knot size leads to an asymptote in the RMSE using starting at around 700 knots.

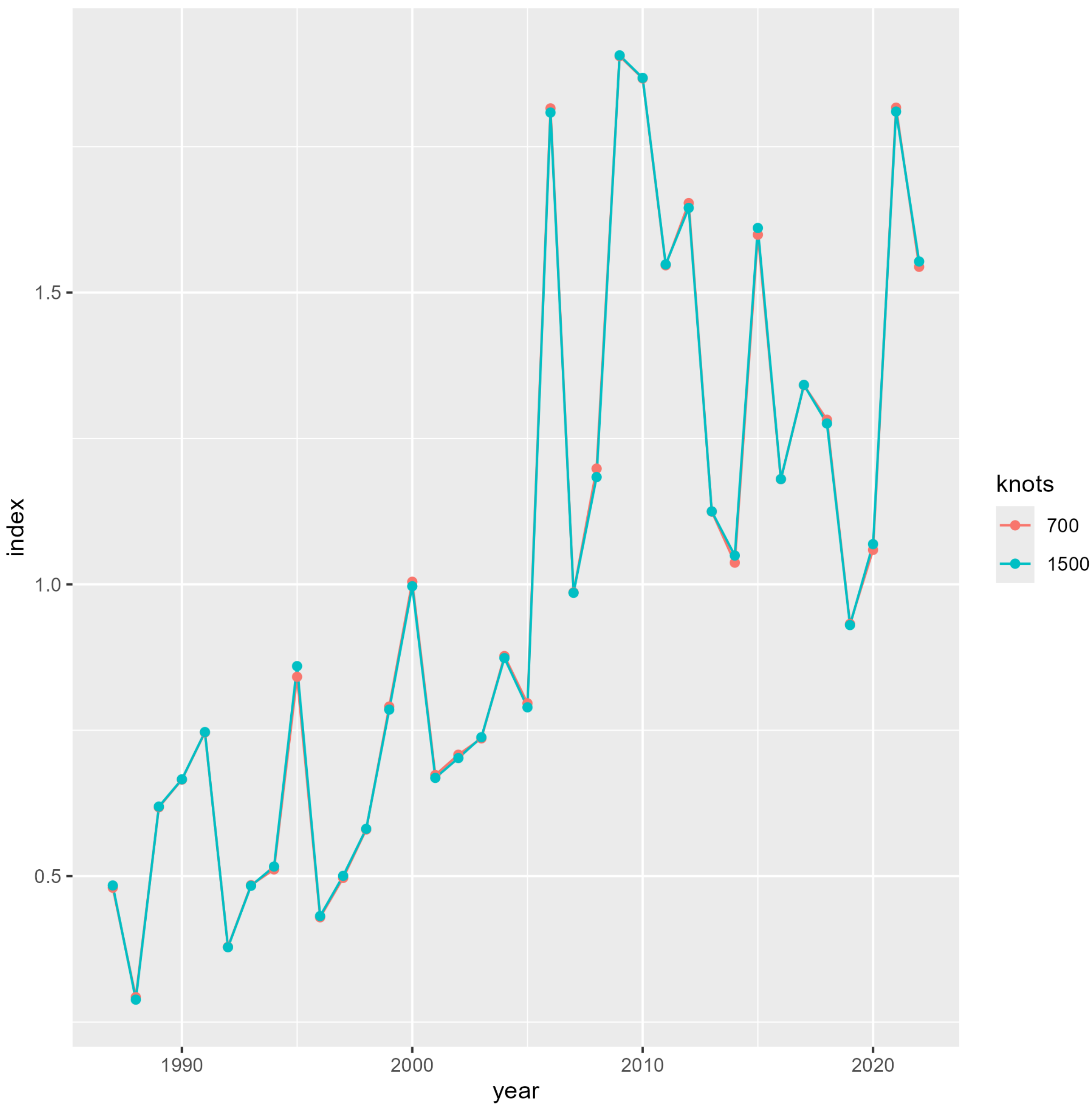


Figure 5: Index estimates for the model run with the highest number of knots (1500) compared with those for the selected model (700).

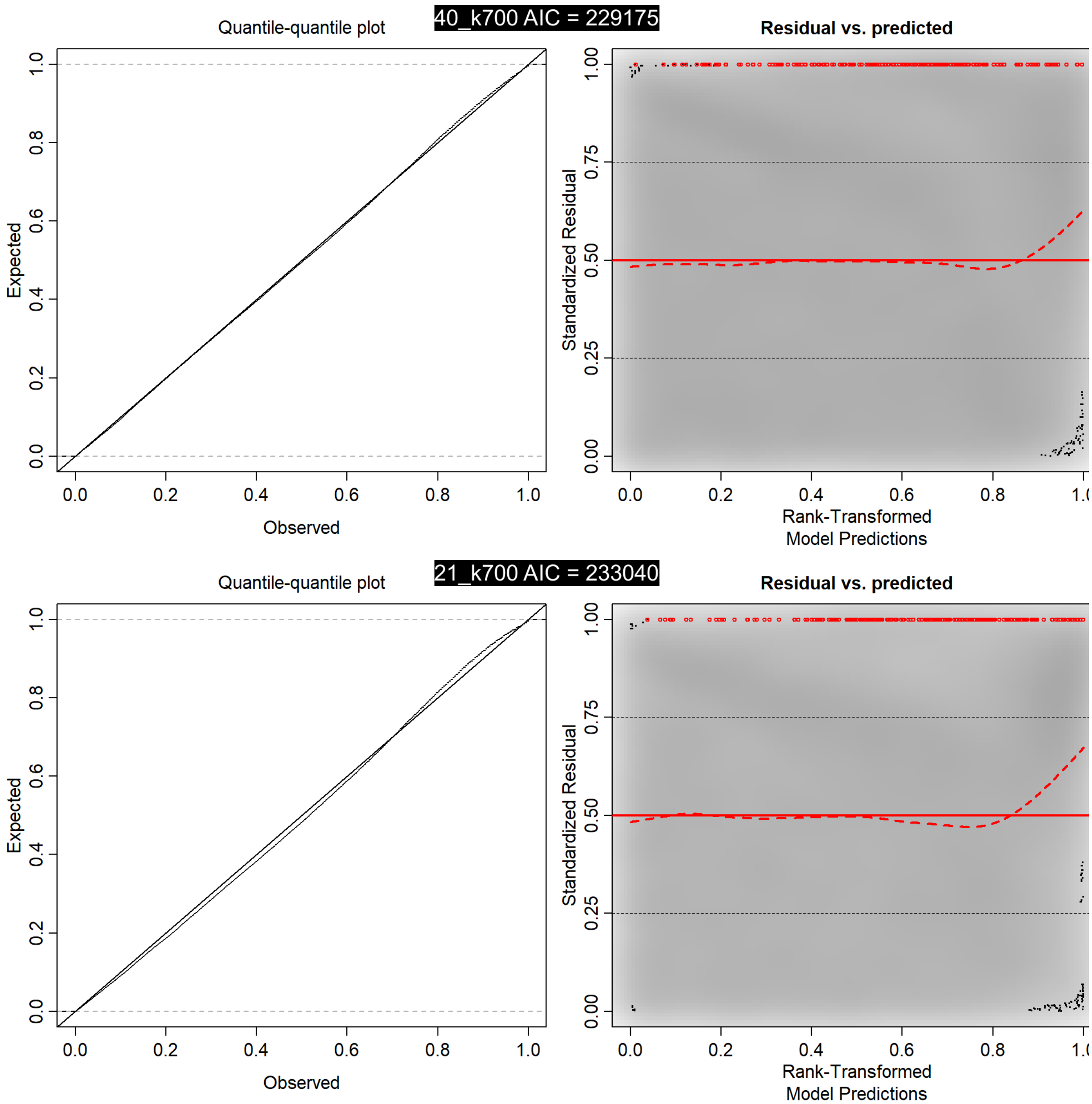


Figure 6: Dharma residual diagnostic plots for the delta-lognormal (top; AIC=229,175) and poisson-link (bottom; AIC=233,040) model.

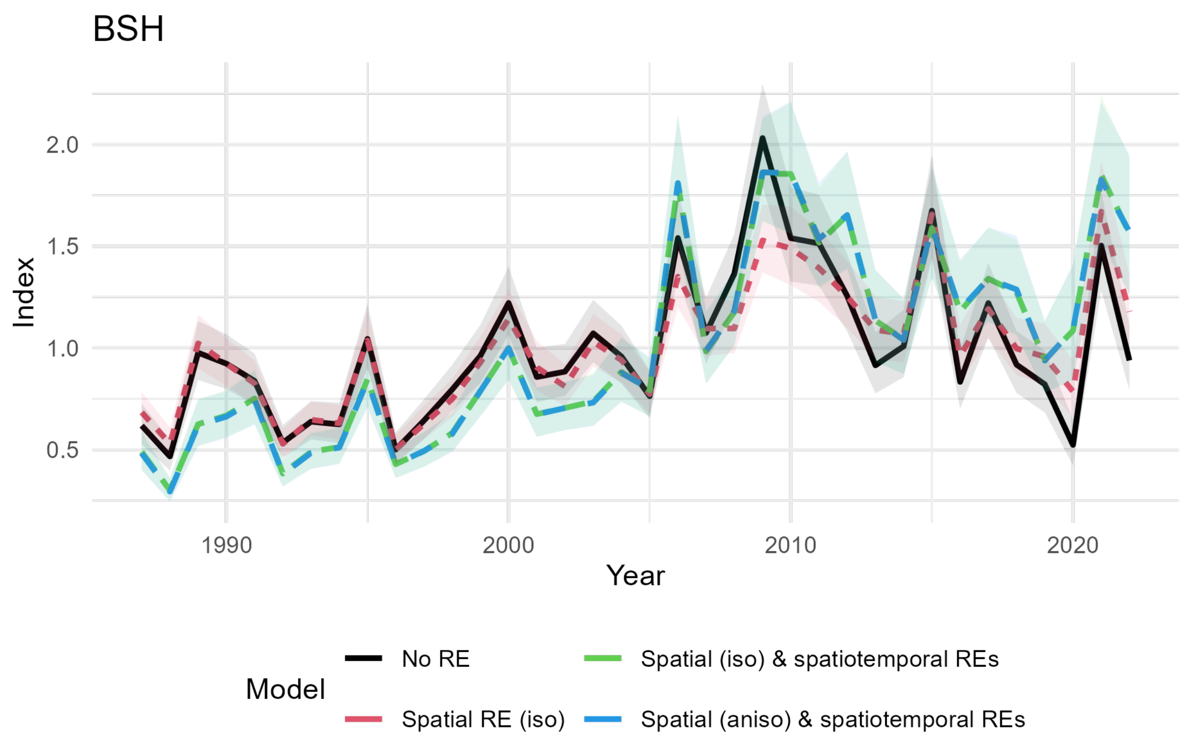


Figure 7: Comparing index estimates and associated confidence intervals across runs with different spatial and spatiotemporal random effects (RE) specifications. iso: isotropic Matérn covariance function; aniso: anisotropic Matérn covariance function.

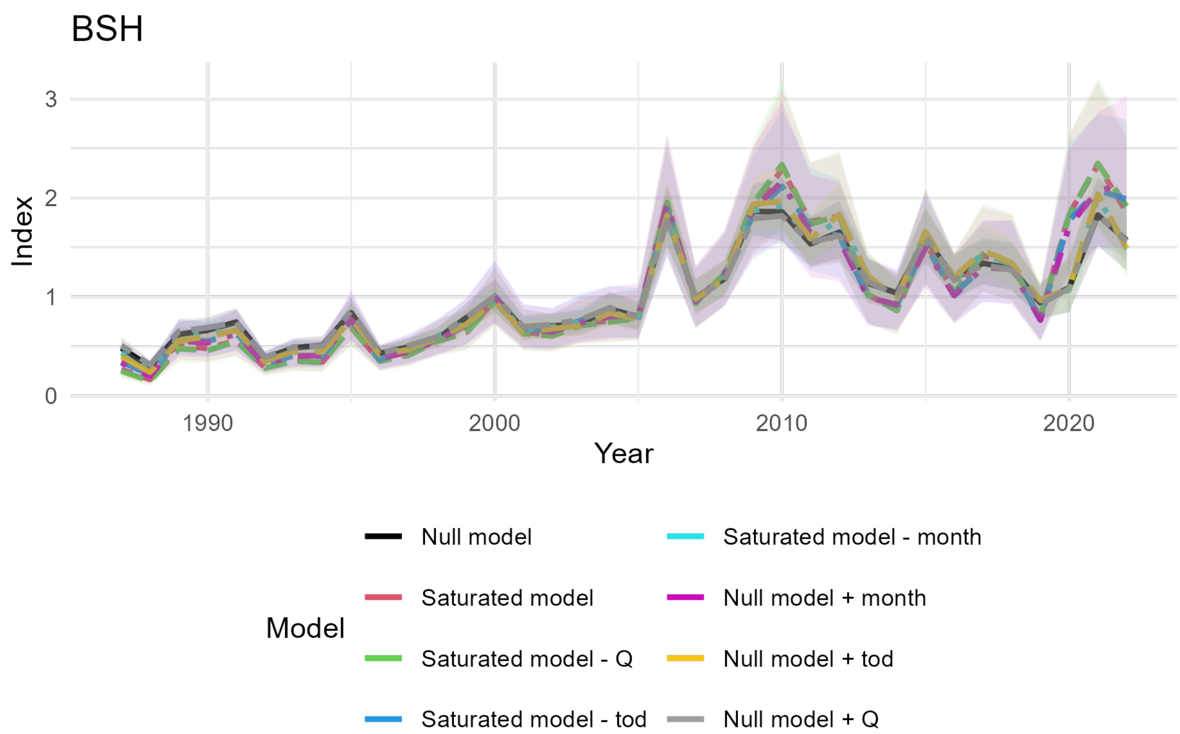


Figure 8: Comparing index estimates and associated confidence intervals across runs with different catchability covariates. The Null model is a model with both spatial and spatiotemporal random effects included in both the 1st and 2nd linear predictors and assuming geometric anisotropy but with no catchability covariates included. tod = time of day (i.e., night vs. day), Q = survey (i.e., TPWD vs. SEAMAP).

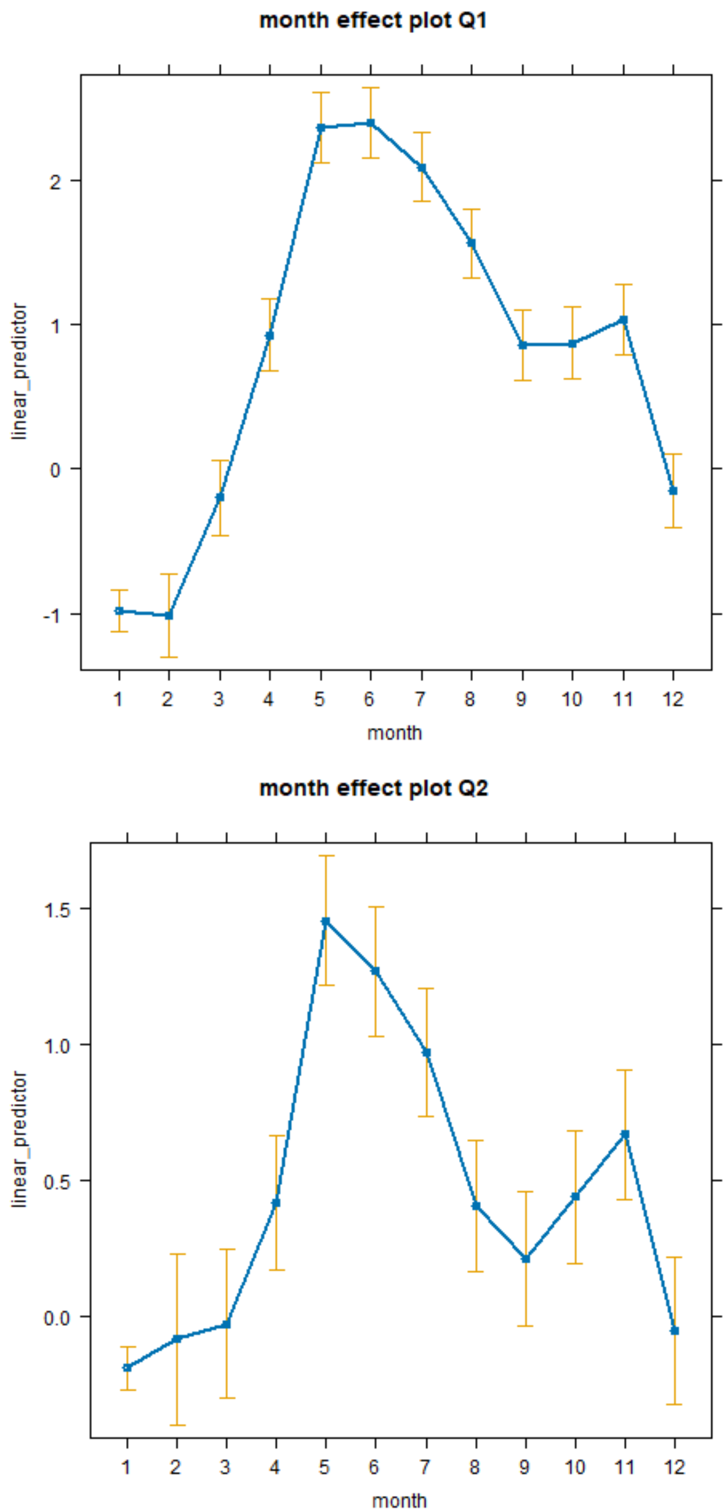


Figure 9: Effect plots for the catchability covariate month. Top panel shows the impact on the first linear predictor, bottom panel shows the impact on the second linear predictor.

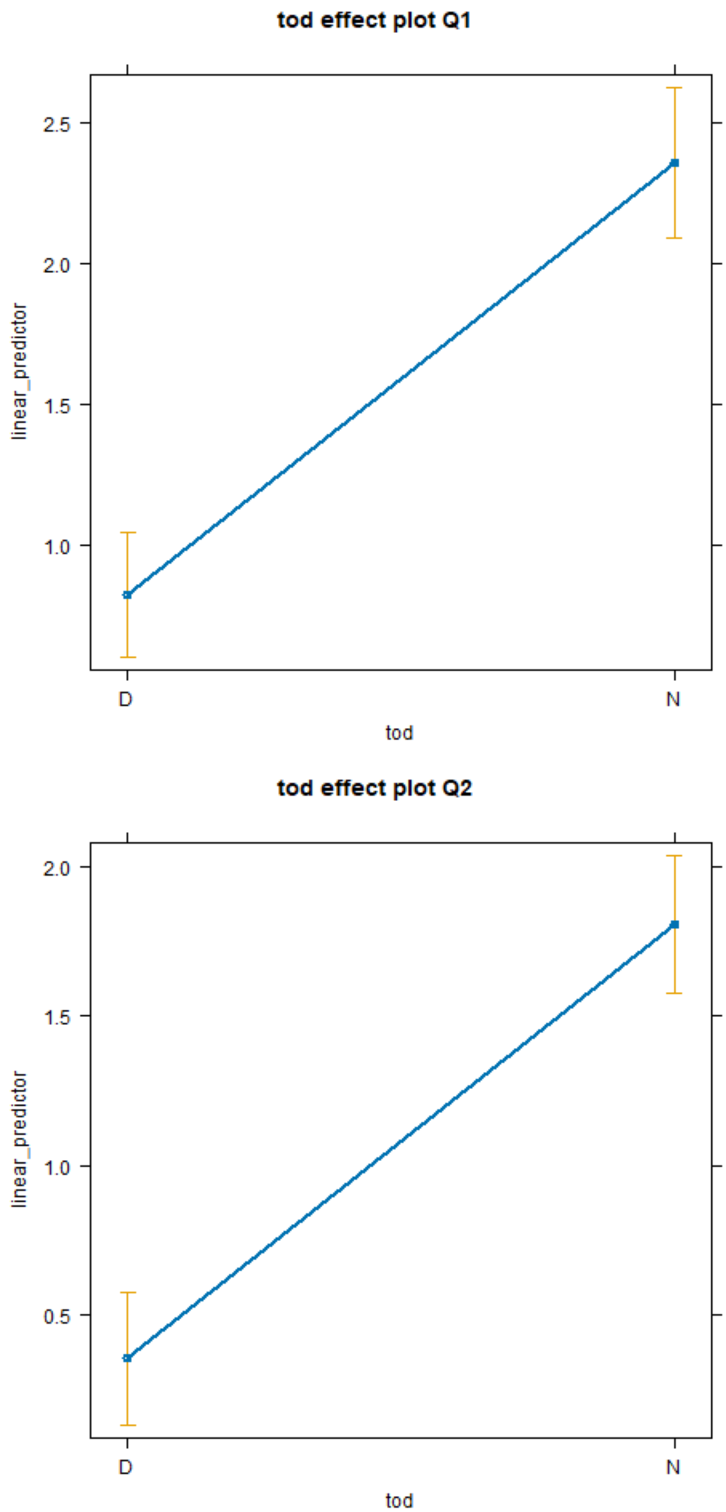


Figure 10: Effect plots for the timem of day catchability covariate. Top panel shows the impact on the first linear predictor, bottom panel shows the impact on the second linear predictor.

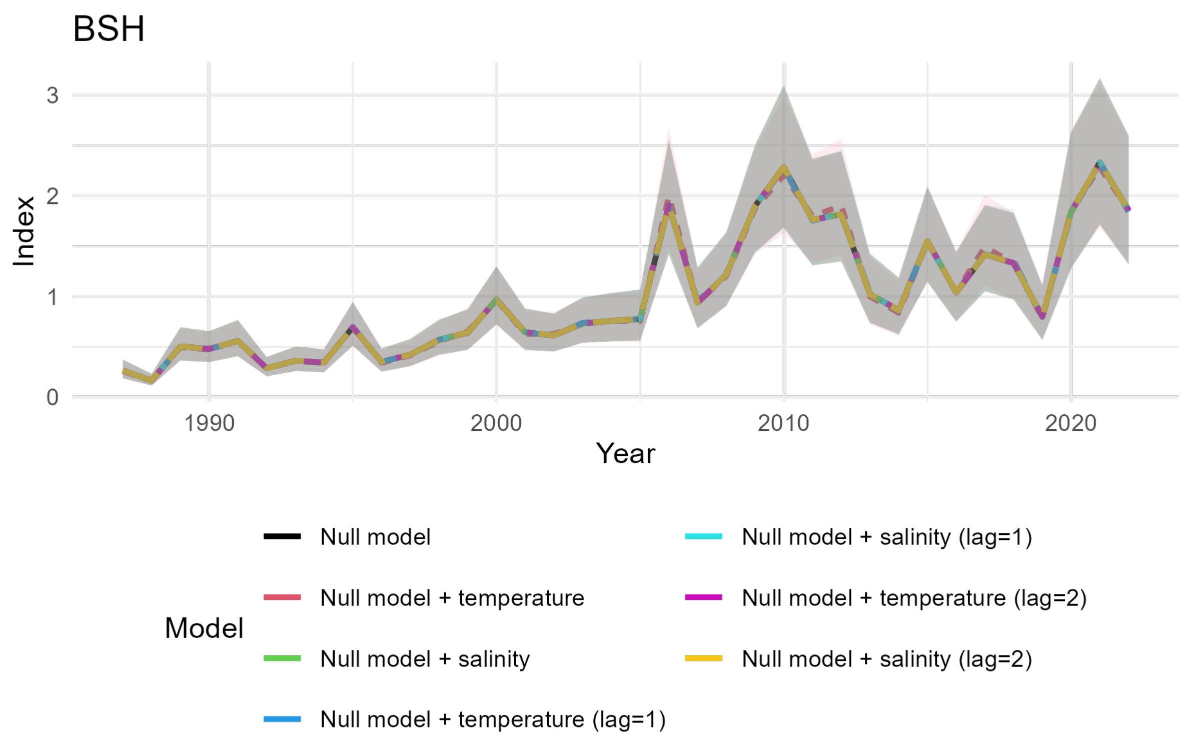


Figure 11: Comparing index estimates and associated confidence intervals across runs with different habitat covariates included. The Null model includes both spatial and spatiotemporal random effects (assuming geometric anisotropy) and catchability covariates for time of day, month and survey. temperature = mean annual temperature on the nursery grounds, salinity = mean annual salinity on the nursery grounds, environmental indices are lagged by 0, 1 or 2 years compared with the cpue observations.

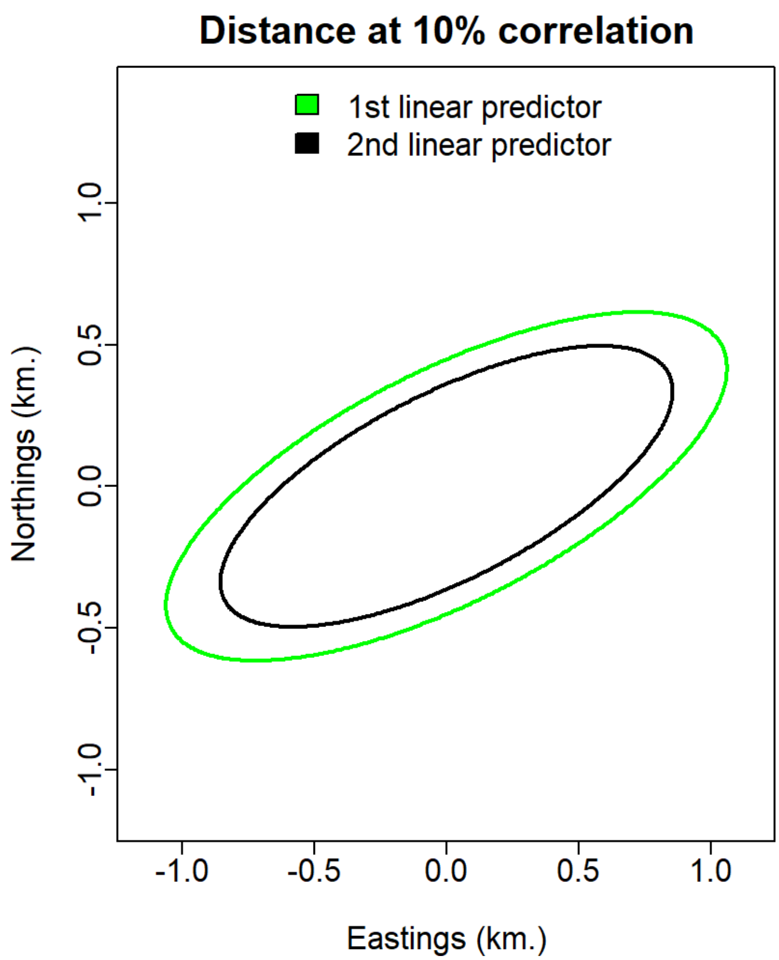


Figure 12: Distance needed to achieve a correlation of approximately 10% from a location centered at coordinates (0,0). Correlations decline slower along the southwest-northeast axis than along the northwest-southeast axis.

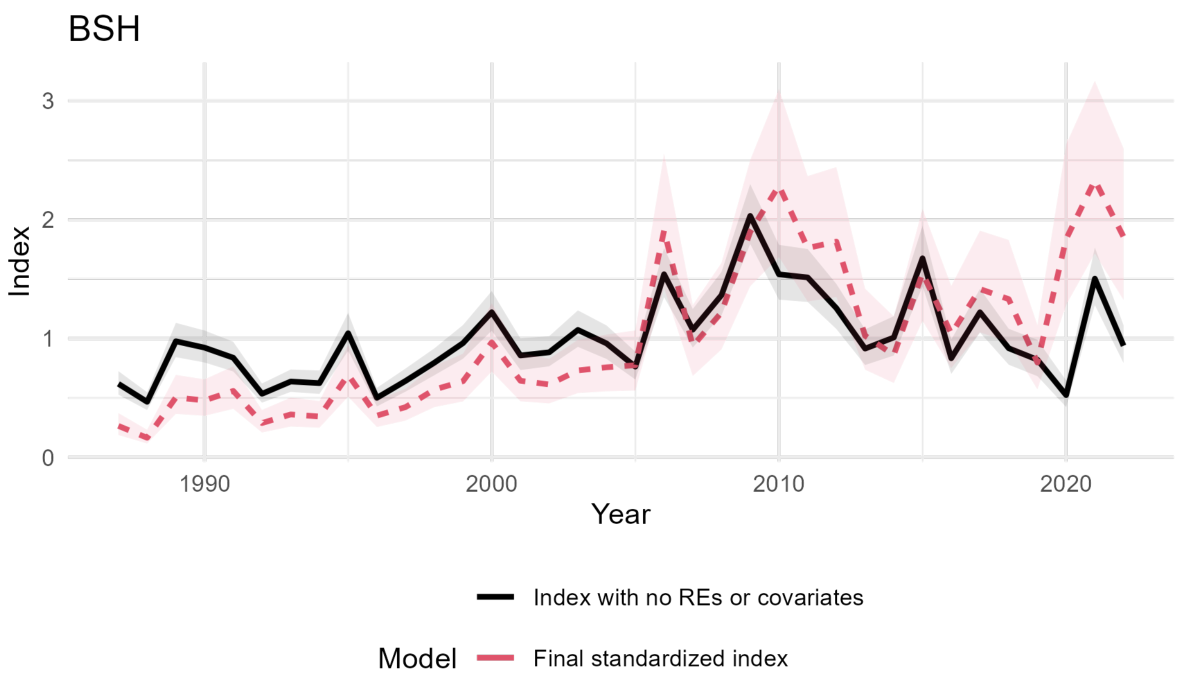


Figure 13: Comparing index estimates and associated confidence intervals for the final model (red) with the preliminary unstandardized index (black). The final index includes both spatial and spatiotemporal random effects assuming geometric anisotropy and catchability covariates for time of day, month and survey.

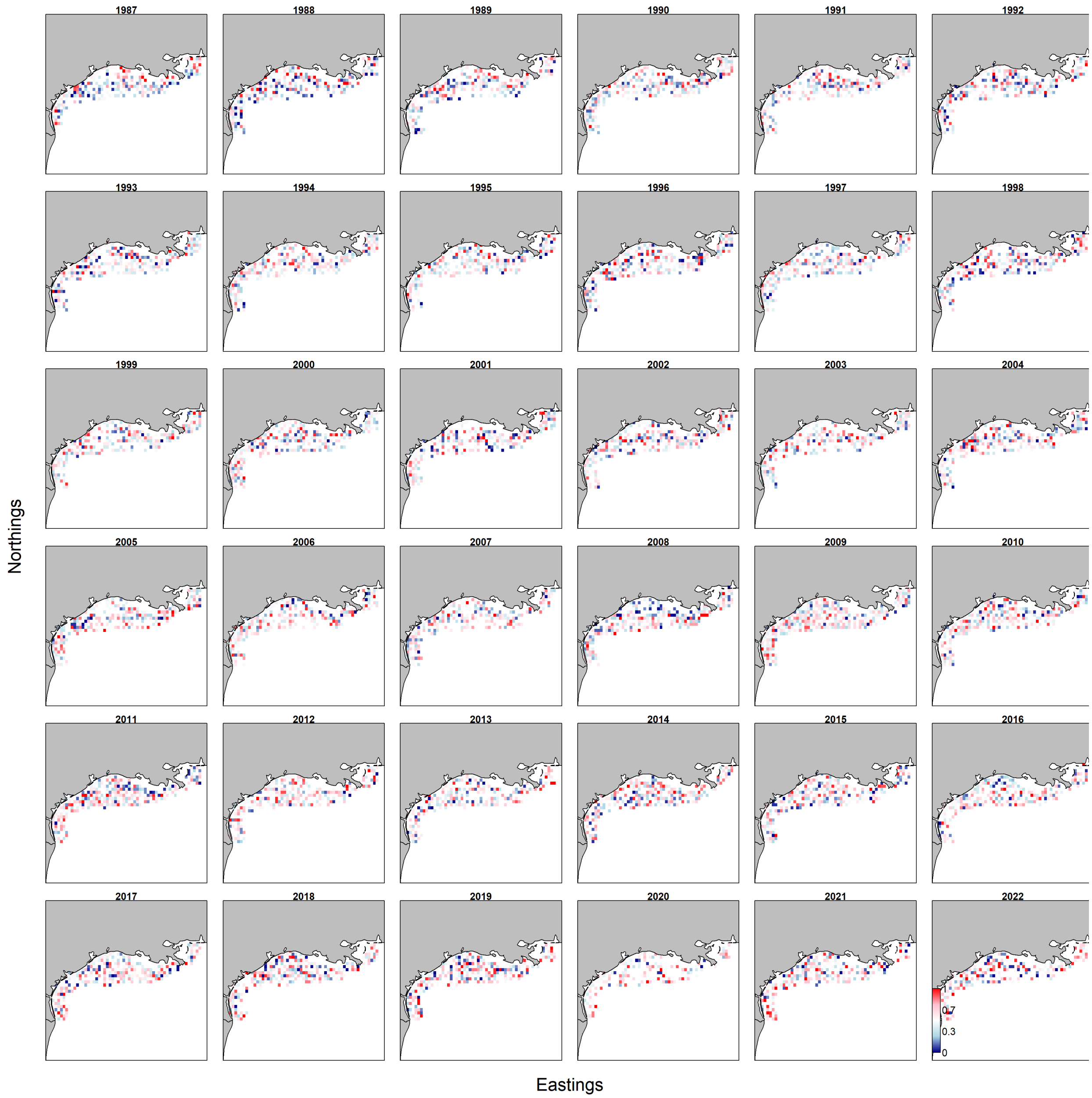


Figure 14: Spatial distribution of quantile residuals for the final model, red color indicating overestimation and blue indicating underestimation.

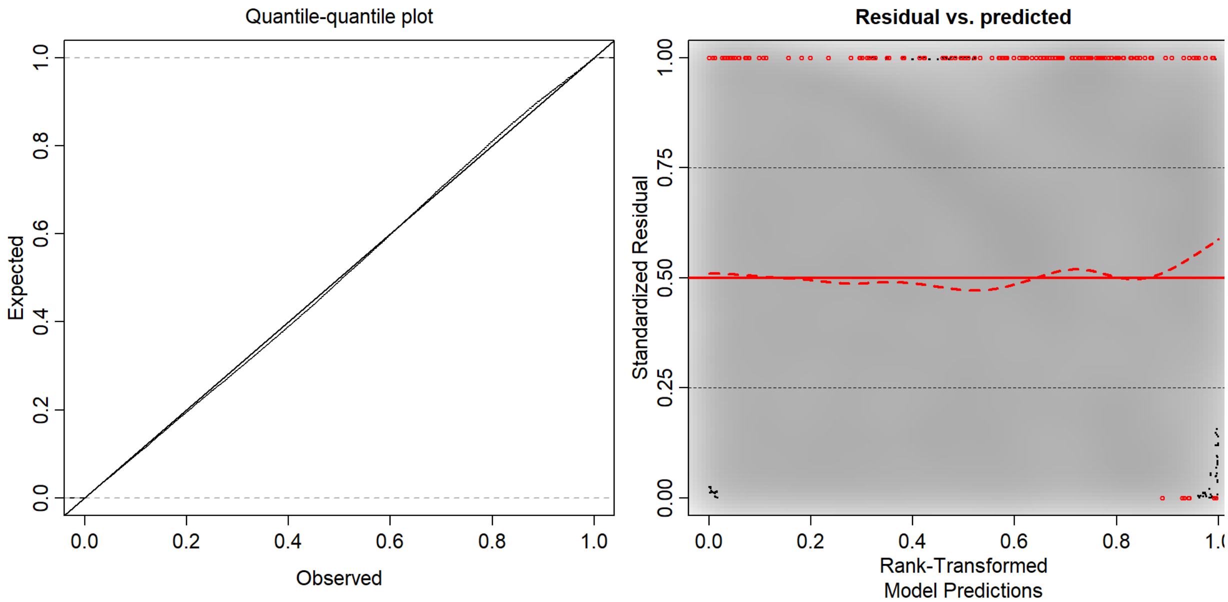


Figure 15: Dharma residual diagnostic plots for the final model.

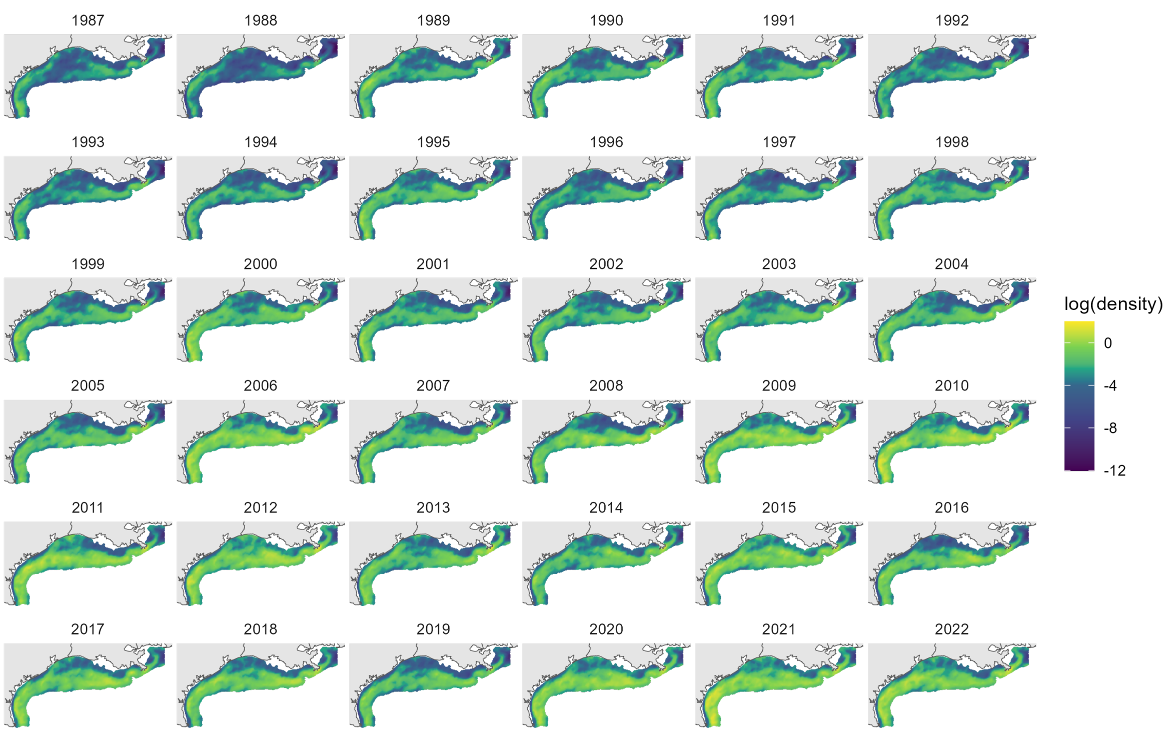


Figure 16: Predicted densities in each year for the final model. The absolute scale is not directly interpretable since no meaningful area swept estimates were available for the development of the index.